Modeling and Simulation of Two Passive Feedback Methods to Obtain Large Travel Range of Electrostatic Micro Mirrors

XingTao Wu*, ZhiXiong Xiao*, Jiang Zhe** and K. R. Farmer*

* New Jersey Institute of Technology, Microelectronics Research Center
Newark, NJ, 07012, USA, xxw3135@njit.edu
** Department of Mechanical Engineering, Columbia University, New York, NY, 10027

ABSTRACT

This paper demonstrates two passive feedback methods to obtain increased travel range in electrostatic micro actuators directly in the *electrostatic* domain. The first method is modeled as a series capacitor loop in which an integrated fixed capacitor is utilized as a voltage divider to control the effective actuation voltage across the variable capacitor/actuator, and the resulting increased travel ranges are obtained up to 100% and ~70% full scale for vertical Z micro actuators and torsion full-plate micro actuators, respectively. The second method utilizes negative feedback due to coulombic repulsion force between the net oxide charges that exist in two oxide layers placed between the actuator electrodes, and the resulting travel range is found to be 62% for a fabricated three-spring device.

Keywords: Electrostatic Micro Mirror, Electrostatic Micro Actuator, Travel Range, Series Capacitor Loop, Pull In.

1 INTRODUCTION

Large travel range is especially important in emerging optical micro mirror and variable capacitor applications. In theory, the maximum travel range before pull in is 33.33% for full-plate vertical out-of-plane electrostatic actuators and 44.04% for torsion electrostatic actuators with full plate electrode [1]. Generally, in order to extend an actuator's travel range before snap down, a negative feedback mechanism is required. *Mechanical* approaches such as leveraged bending and strain stiffening have been examined previously [2]. The two methods described here introduce negative feedback and extend the travel range directly in the *electrostatic* domain. These methods are passive in that no external closed loop feedback control is employed.

The first method utilizes a series capacitor to modulate the effective actuation voltage across the variable capacitor. The resulting voltage across the actuator exhibits a maximum value at a specific applied bias, beyond which it begins to drop even though the charge density keeps increasing to give an increased electrostatic torque. The effect of this decreasing voltage is to delay the increase of electrostatic torque so that the restoring elastic torque can balance it at an expanded travel range. Two typical micro mirror structures, out-of-plane vertical and torsion, are used to verify this concept. In this paper we will first present the mathematical analysis of the series capacitor loop model, then simulation results obtained using the CoSolver feature of Memcad ™ software are compared with analytical results with good agreement.

The second method utilizes negative feedback due to coulombic repulsion between the net oxide charges that exist in two oxide layers placed between the actuator electrodes. The net oxide charge is modeled to be immobile and located within 25Å of the Si-SiO_2 interface, without electrical communication with the Si. The C-V characteristics of the fabricated torsion mirror structure show a negative net oxide charge density of magnitude $10^{10\text{-}12}/cm^2$. The repulsive interaction will occur significantly when oxides layers are in close proximity (e.g. d=6.96μm for our example device). In addition, the fixed charge density is comparable to the surface charge density ($10^{9\text{-}12}/cm^2$) due to applied bias voltage from 1V to 200V for our prototype device. Therefore an extra repulsive electrostatic torque is superimposed on the attractive electrostatic torque to retard the increasing rate of the total electrostatic torque in such a manner that a negative feedback mechanism is introduced into the actuator structure that enables the elastic torque of spring structure to balance the electrostatic torque at an expanded travel range, up to 62% of full scale deflection. This increased travel range occurs at the expense of an increased bias voltage. It should be mentioned that the oxide layers also serve as a voltage divider in the prototype structure, but this effect is not dominant.

2 MODELING AND ANALYSIS FOR METHOD 1

As modeled in Figure 1, the first travel range extension method utilizes an integrated fixed series capacitor as a voltage divider to modulate the effective voltage across the variable capacitor /actuator. Applying Newton's second law to the 1-D actuator system gives the structural equation (1). Differentiating with respect to x, multiplying by x and subtracting equation 1 givens the pull-in equation (2).

$$\frac{1}{2}\frac{dC}{dx}V^2 = Kx \qquad (1)$$

$$\frac{d^2C}{d^2x_{PIN}} - \frac{1}{x_{PIN}}\frac{dC}{dx_{PIN}} = 0 \qquad (2)$$

In these equations C is the overall capacitance of the actuator system and K and x are the generalized spring stiffness and the change of generalized displacement, respectively.

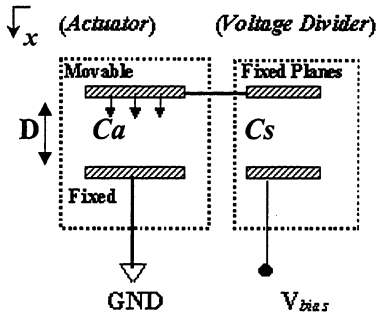

Figure 1: Circuit of Series Capacitor Loop

The static characteristics of an arbitrary electrostatic micro actuator are determined by the 1st and 2nd derivatives of the overall capacitance of the actuator system with respect to x, and the design of an actuator system is simply the design of its overall capacitance. For most applications, there are analytical expression or empirical approximation for the overall capacitance that enable designers to obtain quick characteristics for the static behavior of an electrostatic micro actuator by utilizing the above equations. Now we address the obtainable large travel range for two popular electrostatic micro mirror structures.

2.1 Vertical Z Actuator

In the vertical Z actuator, the movable plate is rigid and suspended by a folded spring structure. We assume that no deformation occurs on the movable electrode plate during actuation as illustrated in figure 2. Also, we consider the case of full plate actuation.

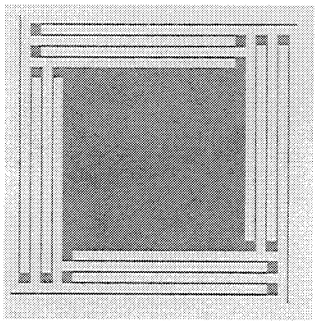

Figure 2: Vertical Z Mirror 2-D layout View

Referring to figure 1, if we define the capacitance ratio $\alpha = C_{a0}/C_s$ (where C_{a0} is C_a at $x=0$), then C_s takes the form: $C_s = \alpha^{-1}C_{a0} = \alpha^{-1}(\varepsilon_0 A/D)$. Considering this integrated capacitance, the net capacitance of the actuator system satisfies the relation $C^{-1} = C_a^{-1} + C_s^{-1}$. The overall capacitance C can be shown to be:

$$C = \frac{\varepsilon_0 A}{(1+\alpha)D - x} \qquad (3)$$

Plugging the 1st and 2nd order derivatives of equation (3) into equation (1) and (2), the structural and pull in equations are obtained as:

$$\frac{\varepsilon_0 A V^2}{2[(1+\alpha)D - x]^2} = Kx \qquad (4)$$

$$\frac{2}{[(1+\alpha)D - x_{PIN}]} - \frac{1}{x_{PIN}} = 0 \qquad (5)$$

The travel range is solved to be:

$$TR = \frac{x_{PIN}}{D} = \frac{1}{3}(1+\alpha) \qquad (6)$$

Thus the effect of the incorporated capacitance is equivalent to a gap depth extension from D to $(1+\alpha)D$. The travel range of the new system becomes 1/3 multiplied by $(1+\alpha)$, always larger than that of a single capacitor system for $\alpha \neq 0$. A ratio $\alpha = 2$ leads to 100% gap depth travel range, where the series capacitance is equal to half of the zero deflection C_{a0} value.

The corresponding pull in voltage is obtained as:

$$V_{PIN} = \sqrt{\frac{8KD^3}{27\varepsilon_0 A}(1+\alpha)^3} \qquad (7)$$

Equation (7) indicates that the increased travel range is obtained at a sacrifice of actuation voltage by a factor of $(1+\alpha)^{3/2}$. Equation (6) at $\alpha = 0$ leads to the well-known 1/3 travel range for a single capacitor vertical z-actuator.

2.2 Cantilever Torsion Actuator

For the wedge shaped capacitance of the actuator shown schematically in figure 3 and considering the single active wedge-like capacitance:

$$C_a = \frac{\varepsilon_0 W}{\theta}\ln\frac{D}{D - L\theta} \qquad (8)$$

where W and L are the mirror width and length respectively, D is initial gap depth and θ is the angle of tilt under bias voltage. In this system the introduction of a series capacitor leads to the ratio $\alpha(\theta)$ such that

$\left[\alpha(\theta)^{-1}-1\right]=C_a(\theta)/C_s$. The overall capacitance C of the torsion actuator system can be easily expressed as: $C=C_a(\theta)\cdot\alpha(\theta)$. For this system, the structural and pull-in equations become:

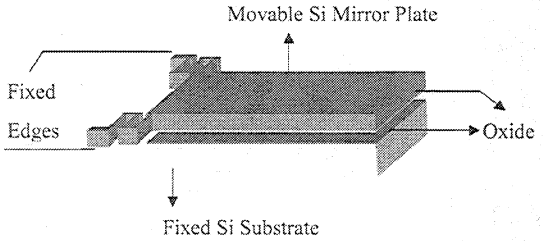

Figure 3: Torsion Micro Mirror with Oxides

$$\frac{1}{2}\left(C_a'\alpha+C_a\alpha'\right)V^2=K_\theta\theta \tag{9}$$

$$\left[\left(C_a''\alpha+2C_a'\alpha'+C_a\alpha''\right)-\frac{1}{\theta}\left(C_a'\alpha+C_a\alpha'\right)\right]_{\theta_{PIN}}=0 \tag{10}$$

The complexity of the capacitance expression requires numerical iteration in order to solve equations (9) and (10). Section 4 will provide a comparison between these solutions and FEA simulation results. It can be shown that for the example device NC3, the travel range increases up to 70% of the full scale deflection.

3 ANALYSIS OF METHOD 2

For the torsion actuator of figure 3, the structural equation is:

$$M^{(A)}(\theta)-M^{(R)}(\theta)=K_\theta\theta \tag{11}$$

$M^{(A)}(\theta)$ and $M^{(R)}(\theta)$ are the electrostatic attractive and repulsive torques respectively. The pull-in angle and bias voltage are determined by solving equation (6):

$$\left(\theta\cdot\frac{dM^{(A)}(\theta)}{d\theta}-M^{(A)}(\theta)\right)-\left(\theta\cdot\frac{dM^{(R)}(\theta)}{d\theta}-M^{(R)}(\theta)\right)=0 \tag{12}$$

Numerical approximation by expansion techniques and FEA simulation can be used to find the solutions for equations (11) and (12).

4 SIMULATIONS AND CALCULATIONS FOR METHOD 1

4.1 Vertical Z Actuator

For vertical bending actuators, as shown in figure 4, the resultant voltage across the actuator exhibits a maximum value at a specific applied bias, beyond which it begins to drop. It can be seen from this calculation that the maximum effective voltage occurs exactly at the original pull in position if no series capacitor were presented. Although the charge density on the movable plate always increases with the bias voltage, the voltage across the air gap does not increase beyond the maximum value because of the rapid capacitance increase of the variable capacitor.

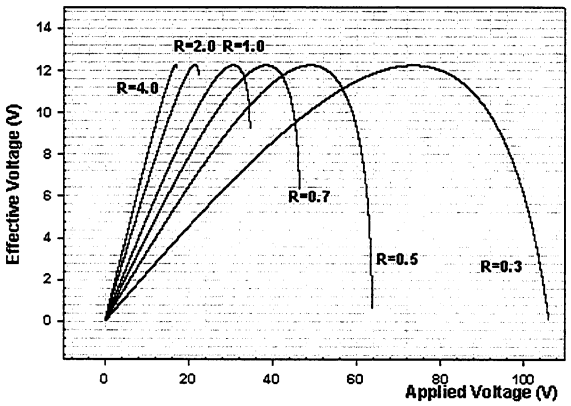

Figure 4: Effective Actuation Voltage vs. Applied Bias Voltage for Different Capacitance Ratio (R=Cs/Cao) for Vertical Z Actuator

The effect of this decreasing voltage is to delay the increase of electrostatic torque so that the restoring elastic torque can balance it at an expanded travel range. Numerical analysis shows that at the expense of increased applied voltage, the series capacitor can expand the travel range to 100% full scale for out-of-plane vertical full-plate micro actuators. The extended travel range (vertical (VC1) devices) is illustrated in figure 5 showing the travel range extension results for different ratios of the series to initial actuator capacitance.

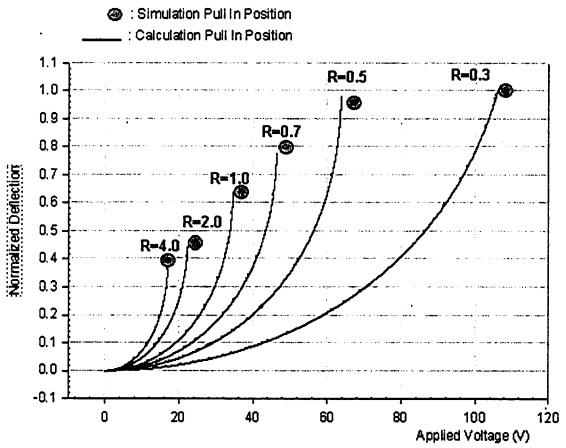

Figure 5: Normalized Deflection vs. Applied Voltage for Different Capacitance Ratios. Vertical Z Actuator VC1 with Gap Depth=4um

In figure 5, R is the reciprocal of the pre-defined capacitance ratio α. The theoretical analysis results agree

very well with simulated results. If R is chosen smaller than 0.5, the full-scale travel range can be achieved.

4.2 Cantilever Torsion Actuator

A torsion mirror (NC3) as illustrated in figure 3, neglecting the effects of oxides, is simulated with different capacitance ratios. Figure 6 shows the comparison of iteration and simulation results, where R is equal to Cs/Ca0. These results are found to be in good agreement.

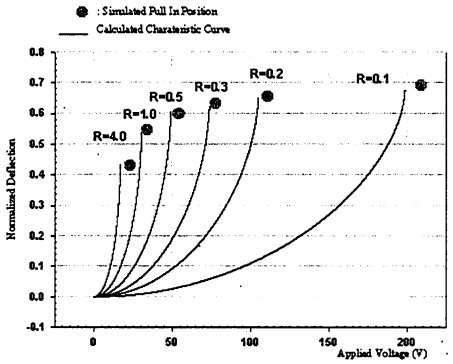

Figure 6: Normalized Deflection vs. Applied Voltage for NC3 Torsion Mirror with Gap Depth=12um.

5 SIMULATION VS EXPERIMENT COMPRISON FOR METHOD 2

For a fabricated torsion actuator of figure 3, the net oxide charge density is calculated to be ~ 6.2 $\times 10^{10}/cm^2$ by C-V characteristics [3]. An empirical expression for repulsive electrostatic torque is curve fitted using equation (7). The resulting expression is given in equation (13). Other devices follow the same pattern with variable coefficients; this fact implies that the net oxide charge has well-defined bias voltage dependence. V_0 (12V for device D3) is the bias voltage at which the mirror has zero deflection angle.

$$M^{(R)}(\theta) = \frac{\varepsilon_0 W (V + V_0)^2}{2}\left(\frac{L}{d}\right)^2\left(0.366 - 0.076\theta + 0.508\theta^2 + 2.23\theta^3\right) \quad (13)$$

The simulated results, and the measured results without the effects of the net oxide charge present, are compared in figure (7). The travel range of D3 was increased from 44% to 62% at the cost of an increased bias voltage.

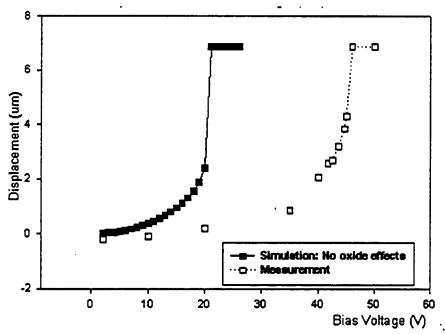

Figure 7: The Measured Effects of Oxides on The Deflection Dependence on Bias Voltage for D3 Device.

6 CONCLUSIONS

Two passive feedback methods have been described which give increased travel range in electrostatic actuators but sacrifice bias voltage. These methods can be combined to optimize travel range for customized applications. Because of their simplicity, reproducibility and ease of manufacture, the methods may be preferred over other travel range extension methods in some electrostatic micro actuator applications, for example, variable capacitors of wide tunable range and large deflection micro mirror structures. Future work needs to be done to investigate the voltage-dependence of net oxide charge and its effects on repulsive electrostatic torque.

This work was supported in part by the New Jersey Commission on Science and Technology through the NJ MEMS Initiative, and by the National Foundation through grant number DMR-9871272.

REFERENCES

[1] Ofir Degani, et al., JMEMS, Vol. 7, No. 4, pp. 373-379, 1998.

[2] Elmer S. Hung, et al., JMEMS, Vol. 8, No. 4, pp. 497-505, 1999.

[3] X.T Wu, et al., OMEMS'2000 Conference Proceeding, IEEE, pp. 151-152.